frontiers in Human Neuroscience

ORIGINAL RESEARCH
published: 14 September 2016
doi: 10.3389/fnhum.2016.00454

Causal Interactions between Frontal$^{\theta}$ – Parieto-Occipital$^{\alpha 2}$ Predict Performance on a Mental Arithmetic Task

Stavros I. Dimitriadis[1,2,3,4], Yu Sun[5], Nitish V. Thakor[5] and Anastasios Bezerianos[5]**

[1] *Institute of Psychological Medicine and Clinical Neurosciences, Cardiff University School of Medicine, Cardiff, UK,* [2] *Cardiff University Brain Research Imaging Center, School of Psychology, Cardiff University, Cardiff, UK,* [3] *Artificial Intelligence and Information Analysis Laboratory, Department of Informatics, Aristotle University of Thessaloniki, Thessaloniki, Greece,* [4] *Neuroinformatics.Group, Department of Informatics, Aristotle University of Thessaloniki, Thessaloniki, Greece,* [5] *Singapore Institute for Neurotechnology, Centre for Life Sciences, National University of Singapore, Singapore, Singapore*

Many neuroimaging studies have demonstrated the different functional contributions of spatially distinct brain areas to working memory (WM) subsystems in cognitive tasks that demand both local information processing and interregional coordination. In WM cognitive task paradigms employing electroencephalography (EEG), brain rhythms such as θ and α have been linked to specific functional roles over given brain areas, but their functional coupling has not been extensively studied. Here we analyzed an arithmetic task with five cognitive workload levels (CWLs) and demonstrated functional/effective coupling between the two WM subsystems: the central executive located over frontal (F) brain areas that oscillates on the dominant θ rhythm (Frontal$^{\theta}$/F$^{\theta}$) and the storage buffer located over parieto-occipital (PO) brain areas that operates on the α_2 dominant brain rhythm (Parieto-Occipital$^{\alpha 2}$/PO$^{\alpha 2}$). We focused on important differences between and within WM subsystems in relation to behavioral performance. A repertoire of brain connectivity estimators was employed to elucidate the distinct roles of amplitude, phase within and between frequencies, and the hierarchical role of functionally specialized brain areas related to the task. Specifically, for each CWL, we conducted a) a conventional signal power analysis within both frequency bands at F$^{\theta}$ and PO$^{\alpha 2}$, b) the intra- and inter-frequency phase interactions between F$^{\theta}$ and PO$^{\alpha 2}$, and c) their causal phase and amplitude relationship. We found no significant statistical difference of signal power or phase interactions between correct and wrong answers. Interestingly, the study of causal interactions between F$^{\theta}$ and PO$^{\alpha 2}$ revealed frontal brain region(s) as the leader, while the strength differentiated between correct and wrong responses in every CWL with absolute accuracy. Additionally, zero time-lag between bilateral F$^{\theta}$ and right PO^{a2} could serve as an indicator of mental calculation failure. Overall, our study highlights the significant role of coordinated activity between F$^{\theta}$ and PO$^{\alpha 2}$ via their causal interactions and the timing for arithmetic performance.

Keywords: working memory, cognition, cross-frequency coupling, mental arithmetic, hierarchical organization

OPEN ACCESS

Edited by:
Yong He,
Beijing Normal University, China

Reviewed by:
Xin Di,
New Jersey Institute of Technology, USA
Sahil Bajaj,
University of Arizona, USA

****Correspondence:***
Stavros I. Dimitriadis
dimitriadiss@cardiff.ac.uk;
stidimitriadis@gmail.com
Anastasios Bezerianos
tassos.bezerianos@nus.edu.sg

Received: *25 March 2016*
Accepted: *26 August 2016*
Published: *14 September 2016*

Citation:
Dimitriadis SI, Sun Y, Thakor NV and Bezerianos A (2016) Causal Interactions between Frontal$^{\theta}$ – Parieto-Occipital$^{\alpha 2}$ Predict Performance on a Mental Arithmetic Task. Front. Hum. Neurosci. 10:454. doi: 10.3389/fnhum.2016.00454

INTRODUCTION

Based on a psychology theory, the human working memory (WM) system possesses a star topology with the executive element in the center and supportive elements in the periphery. The central executive is the core of the human WM system and controls and organizes information selection and processing. Peripheral WM subsystems store task-relevant information for the short term and can be called buffers (e.g., like a visuospatial sketch of a visual stimulus).

Neuroimaging studies have identified the brain regions involved in accessing these storage systems, providing new anatomic insight for better understanding the coordination of neural activities from multiple brain regions in the WM system (Sauseng et al., 2005; Kawasaki et al., 2010; Zanto et al., 2011). It was previously assumed that the prefrontal cortex (PFC) affects processing in posterior brain regions (Friese et al., 2013; Szczepanski et al., 2014; Harding et al., 2015). This assumption led to the hypothesis that PFC activity should precede parietal activity in cognitive control (Brass et al., 2005). It is generally accepted that top-down signals from frontal areas are important for cognitive control (Desimone and Duncan, 1995; Miller and Cohen, 2001; Corbetta and Shulman, 2002). Frontal activity, specifically in the PFC, is thought to affect posterior regions and facilitate the processing of task-relevant information (Reynolds and Chelazzi, 2004; Maunsell and Treue, 2006). Two time series {X,Y} [e.g., electroencephalography (EEG) oscillations] have a causal relationship when past values of X can be useful for predicting future values of Y. This terminology of causality was first formulated by Granger (1969). The above assumption is supported by the time precedence of prefrontal activity (Brass et al., 2005; Grent-'t-Jong and Woldorff, 2007), synchronization between prefrontal and posterior regions (Buchel and Friston, 1997; Sakai and Passingham, 2003), and modulation of posterior region activity after inactivation of prefrontal regions via transcranial magnetic stimulation (TMS; Taylor et al., 2007).

The causal role of the PFC modulating evoked activity in the extrastriate cortex during experiments related to scenes and faces (Miller et al., 2011) and recent combined TMS/EEG and TMS/functional magnetic resonance imaging (fMRI) studies (Feredoes et al., 2011; Higo et al., 2011; Zanto et al., 2011) clearly supports the idea that the PFC is the source of top-down signals and plays a key role in allocating attentional resources related to semantic long-term memory (e.g., letters, numbers, sounds, and motor or sensory information; D'Esposito and Postle, 2015).

Neural activity and related oscillations can be studied at many levels using spike trains, local field potentials (LFPs), and large-scale oscillatory activity that can be measured with EEG. For large-scale oscillations, amplitude changes due to variable synchronization in a neural ensemble are usually referred to in the literature as local synchronization. Oscillatory activities between distant neural structures (neural ensembles or single neurons) can also be synchronized. Neural synchronization and oscillations with a specific frequency profile have been associated with various cognitive functions like memory, perception, motor control, and information transfer (Fries, 2005; Fell and Axmacher, 2011).

EEG oscillations are thought to reflect the orchestration of cell assemblies via the synchronization of neurons related to specific functions and the activities of many local cell assemblies linked to different functions that are integrated via large-scale synchronization (Varela et al., 2001). This hypothesis is the basis for the use of EEG-dominant oscillations for exploring dynamic functional connectivity (Dimitriadis et al., 2012). Numerous EEG studies using scalp recordings have demonstrated modulated θ and α brain rhythms in anatomically restricted brain regions and simultaneous phase synchronization between them during various WM tasks (Jensen and Tesche, 2002; Mizuhara et al., 2004; Sauseng et al., 2005; Kawasaki and Watanabe, 2007; Klimesch et al., 2008; Kawasaki et al., 2010). Each EEG oscillation is closely related to the functional role of each anatomically distinct brain area linked to one or more separate cognitive functions (Başar et al., 2014). Even though there is a debate about the link between cognitive functions and the dominant interaction type, there is ample evidence that cross-frequency coupling (CFC) based on phase domain may be the substrate that links these frequency-independent cognitive functions (e.g., WM subsystems; Fell and Axmacher, 2011). For instance, Kawasaki et al. (2010) suggested that WM task-relevant brain regions [i.e., Frontal (F) and Parieto-Occipital (PO) regions] are coordinated by an *m*:*n* phase synchronization between θ oscillation (θ, 5–8 Hz) in frontal (F^{θ}) and α_2 oscillation (α_2, 10–13 Hz) at PO regions ($PO^{\alpha 2}$). In a systematic review, Fell and Axmacher (2011) highlighted that phase–amplitude coupling and *m*:*n* phase coupling are crucial for a non-interfering representation of multiple objects in the WM.

Among various WM tasks, mental arithmetic is often used to investigate the neurophysiologic basis of WM. Two studies based on EEG event-related responses for mental subtraction and addition adopted a calculation strategy that highlighted the importance of θ and α oscillations (De Smedt et al., 2009; Grabner and De Smedt, 2011). Moreover, evidence from several neuroimaging studies indicates that several cortical areas distributed over both hemispheres are generally implicated in arithmetic processing (Menon et al., 2000; Gruber et al., 2001; Dehaene et al., 2003, 2004; Kong et al., 2005; Fehr et al., 2007; Ischebeck et al., 2009). For example, multiplication operations demand the retrieval of arithmetic facts (e.g., multiplication tables) that are stored in the verbal memory (manipulation of verbal numbers) and specifically require left angular gyrus activation (Gruber et al., 2001; Dehaene et al., 2003; Ischebeck et al., 2009). In contrast, subtraction and addition demand a calculation where the two numerical quantities must first be represented as quantities, and this process activates regions in the parietal cortex (Chochon et al., 1999; Menon et al., 2000; Dehaene et al., 2003; Fehr et al., 2007). It is important to understand the different roles of each brain area involved in mental arithmetic (Dehaene et al., 2004), their preferred "working" frequencies (Ishii et al., 2014), and possible cross-frequency coordination to obtain a correct outcome (Roux and Uhlhaas, 2014).

In our first attempt, we aimed to differentiate two extreme cognitive workload levels (CWLs): the addition of single-digit

numbers (CWL-1) with three-digit numbers (CWL-5) based on a single-subject dataset. We successfully separated the two CWLs using highly accurate connectivity patterns (Dimitriadis et al., 2013). Based on these promising results, we focused on how to correctly predict any CWL among the five CWLs. We discriminated on a high recognition-rate (96%) the five CWLs by constructing the first functional connectivity graph (FCG) that incorporates intra-frequency phase coupling within frontal and PO brain areas operating on their dominant oscillation (θ and α, respectively) and the inter-frequency phase-to-phase coupling between those two areas. The FCG was analyzed with a tensorial approach (Dimitriadis et al., 2015b). As the next step, we attempted to predict performance in arithmetic calculations based on the previous analysis and a causal relationship between prefrontal and parietal activity in which cognitive control was addressed (Brass et al., 2005). To study causal relations between F^{θ} and $PO^{\alpha 2}$, we introduced a new information-theoretic method based on symbolic transfer entropy that quantifies the strength, direction, and delay of coupling between neural signal activities in different frequency ranges (Dimitriadis et al., 2015d). We found that this method successfully uncovering the leading role of θ band oscillation in F areas over α_2 frequency oscillation in PO at each CWL (Dimitriadis et al., 2016a).

Here we employ these techniques to predict arithmetic performance. The scope of this work was fourfold: (i) to uncover the different roles of amplitude and phase representation of θ and α_2 activity while performing mental calculations, (ii) to study the different types of phase synchronization between F^{θ} and PO WM subsystems, (iii) to address and quantify the causal interactions between the two WM subsystems (F^{θ} and $PO^{\alpha 2}$), and (iv) to investigate how WM subsystems can be coordinated for coherent cognitive function. To address these questions, we analyzed the correct and wrong answers in an EEG arithmetic task (addition) with varying difficulty (Lv; i.e., increasing the numbers of digits in the added numbers). Our hypothesis was based on the model in **Figure 1** where stimulus-related information is stored in the posterior brain areas via the α_2 brain rhythm, while manipulation of the abstract-stored information is manipulated by the frontal executive brain areas under θ rhythm via the cross-frequency coupling pathway (Kane and Engle, 2002).

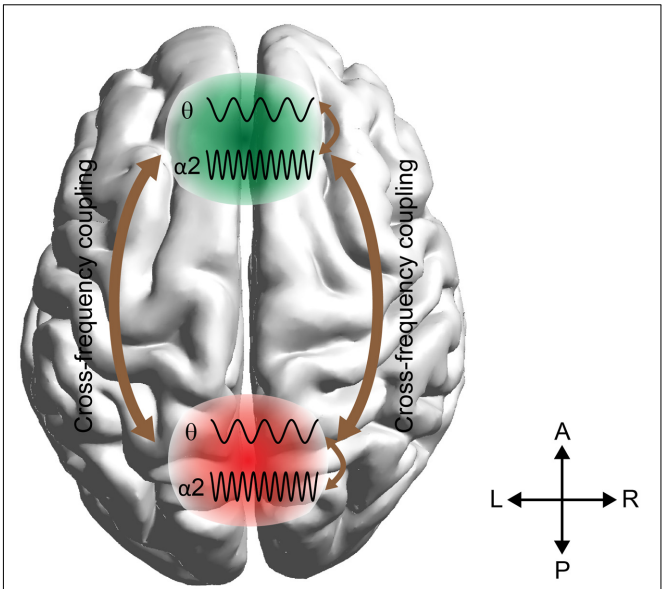

FIGURE 1 | Schematic illustrations of working memory (WM) manipulation of the visual representations. The external visual information is stored in the modality-specific posterior region by the α2 rhythm. For manipulation of the stored representations, the cross-frequency phase coupling (CFPC) between θ–α2 connect the frontal (F) executive regions with parieto-occipital (PO) regions where the visual and number related information is stored. Moreover, θ–α2 interact within both F and PO regions.

MATERIALS AND METHODS

Subjects

We recruited 16 young, right-handed volunteers (nine males and seven females, ages 21–26 years, mean age of 21.5 [$SD = 1.5$ years]) from the National University of Singapore. All participants had normal or corrected-to-normal vision and reported that they did not have verbal or non-verbal learning disabilities. The study was approved by the Institutional Review Board of the National University of Singapore conforming with the Code of Ethics of the World Medical Association (Declaration of Helsinki), and written inform consent was obtained from each participant after the procedures were clearly explained.

EEG Recordings

EEG data were recorded from 64 channels at 256 Hz with an ActiveTwo Biosemi system and referenced using an average reference. The experiment details were described previously (Dimitriadis et al., 2015b, 2016a). Briefly, we asked each participant to perform the mental summation of two numbers presented on a PC screen. When the subject finished the arithmetic task, he/she pressed the spacebar, and two possible answers appeared on the screen. The subject had to compare the mentally calculated summation with the two options. The participant was asked to press either the left or right arrow key (⇐ or ⇒) that corresponded to the correct answer. If the participant responded correctly or incorrectly, the trial was characterized as correct or wrong, respectively. The experiment design included five difficulty levels that differed by the number of digits of the added numbers. For the first level, arithmetic problems involved the summation of two one-digit numbers (e.g., 7 + 9). For each subsequent level, the number of digits of one of the numbers increased by one; therefore, at level five the mental arithmetic task consisted of the summation of two three-digit numbers (e.g., 235 + 164). The experimental paradigm was divided into 1-min with 30-sec rests to avoid cognitive fatigue. All the arithmetic problems within each block had the same difficulty level. After a three repetitions of the five difficulty levels, subjects relaxed by viewing a slide show with landscape pictures with a frequency of 1 picture every 30 sec. We selected landscapes over a fixation cross to increase subject alertness. Then, the whole

session was repeated with 15 blocks of mental arithmetic and 5 min of relaxation. Due to the different response times, each subject performed a different number of trials for each block.

A single trial was defined as the time interval between stimulus onset and the last peak of θ (6 Hz) cycle[1] before the subject pressed the space bar.

Data Preprocessing

We performed independent component analysis (ICA; Onton et al., 2006; Delorme et al., 2007; Romero et al., 2008) to suppress artifactual activity, after first concatenating the trials using the EEGLAB package (Delorme and Makeig, 2004). Independent components (ICs) marked as artifacts (eyes, muscle, and cardiac interference) were zeroed (Dimitriadis et al., 2010). Afterward, we reconstructed the multichannel signal from the non-artifactual ICs using the estimated mixing matrix.

Determining Frequency Bands and Recording Sites of Interest

Previous works (Sauseng et al., 2005; Klimesch et al., 2008; Kawasaki et al., 2010) revealed a distinct role of frequency bands originating from brain areas related to specific cognitive roles in WM and mental arithmetic tasks. Based on this knowledge, we targeted our connectivity analysis to selected brain areas with a characteristic frequency profile. In multiplication and comparison tasks, an increment of θ power over frontal brain areas in both hemispheres and a decrement of power in α_2 frequency over PO sites in both hemispheres were detected for both tasks (Micheloyannis et al., 2005). First, based on preliminary analysis published in our previous study (Dimitriadis et al., 2015b), we demonstrated that higher cognitive loads are linked to: (i) increased power in θ (5–6 Hz) and α_2 (10–13 Hz) frequency bands over F brain areas bilaterally and (ii) increased power in θ and α_2 over PO regions bilaterally (for power spectrum (PS) estimation see Supplementary Material Section 1). Sensors located over bilateral F and PO that demonstrated this tendency in θ (5–6 Hz) and α_2 (10–13 Hz) power, respectively, were selected for further analysis. The selected sensors included FZ, FP1, AF3, F3, F7, FC5, FC1, FC6, FC2, F4, F8, FP2, AF4, PZ, P7, P8, P5, P6, PO7, PO8, PO3, O1, OZ, O2, and PO4.

Different Types of Connectivity Estimators

To uncover the different roles of amplitude and phase on predicting task performance and determine their potential causal relationship within and between different frequencies, we adopted a repertoire of established connectivity estimators and a novel one (Dimitriadis et al., 2016a). Specifically, we employed the phase locking value (PLV; Lachaux et al., 1999), directed phase lag index (dPLI; Stam and van Straaten, 2012), phase-to-amplitude cross-frequency coupling (PAC; Cohen, 2008; Voytek et al., 2010; Dimitriadis et al., 2015a, 2016b; Adamos et al., 2016), and delay symbolic transfer entropy (dSTE; Dimitriadis et al., 2016a).

Within and Cross-Frequency Phase Synchronization between F$^{\theta}$ and PO$^{\alpha 2}$

To quantify the phase interaction within F$^{\theta}$ and PO$^{\alpha 2}$ and also between the two brain areas functioning on their prominent frequency, we adopted *PLV* as an index to quantify phase synchronization on a single-trial basis. The center frequency for θ was 6 Hz, and the range for α_2 was 10–13 Hz (for further details see Supplementary Material Section 2). Briefly, *PLV*s were estimated in a pairwise fashion from the brain signals recorded at sensors *k*, *l* oscillating on prominent frequencies (i.e., θ for F areas and α_2 for PO areas) with the following formula:

$$PLV\left(x_k(f,n), x_l(f,n)\right) = \left| \frac{1}{(W.\Delta s)} \sum_{n'=1}^{W} \sum_{s=s_1}^{s_2} exp\left(i\left(\varphi^{x_k}(f,n',s) - \varphi^{x_l}(f,n',s)\right)\right) \right| \quad (1)$$

Here, $x_k(n)$ denotes a single trial (correct or wrong response) segment of length equal to N_w samples extracted from addition of one of the CWLs. $\Phi_k(s_1,n)$ defines the instantaneous phase for the single-trial segment over N_{s1} scales within either the θ or α_2 frequency bands. W equals the variable width in samples of each trial. Phase estimation via Morlet wavelet transform with a Gaussian envelope in the time domain (characterized by standard deviation σ_t) produced a complex number located at a center frequency f with resolution σ_f ranging from σ_1 to σ_2 (Tallon-Baudry et al., 2001). Then, single-trial phase synchronization was quantified with the *PLV* formula between preselected EEG sensors over F and PO brain sites within θ or α_2 frequency bands (i.e., $PLV({}^{\theta}x_k, {}^{\theta}x_l)$ and $PLV({}^{\alpha 2}x_k, {}^{\alpha 2}x_l)$).

We also estimated the phase-phase cross-frequency coupling between F$^{\theta}$ and PO$^{\alpha 2}$ between every pair of sensors from F and PO brain areas as a coordinated mechanism between the two functionally distinct WM subsystems (i.e., central executive and storage buffer). Adopting the concept of *n*:*m* phase synchronization (Tass et al., 1998), we modified Eq. 1 to estimate the cross-frequency phase-to-phase differences between two cycles of θ phases ($2 \times \Phi_{6Hz}$) and one cycle of the α_2 phase ($\Phi_{10-13\ Hz}$) between the preselected sensors over F and PO brain areas:

$$PLV\left(x_k(f^{\theta},n), x_l(f^{\alpha_2},n)\right) = \left| \frac{1}{(W.\Delta s)} \sum_{n'=1}^{W} \sum_{s=s_1}^{s_2} exp\left(i(2^{*}\varphi_{6Hz}{}^{x_k}(f^{\theta},n',s) - \varphi_{10-13Hz}{}^{x_l}(f^{\alpha_2},n',s))\right) \right| \quad (2)$$

$PLV\ ({}^{f\theta}x_k, {}^{f\alpha 2}x_l)$ quantified the information exchange rate between distinct WM subsystems (for further details – see Supplementary Material Section 2). We previously found that cross-frequency coupling significantly improved the classification

[1] We detected the peaks of θ (6 Hz) cycles by estimating zero crossings from positive to negative values of the derivative of the time series recorded from the FZ sensor and filtered at 6 Hz. The same procedure was employed across trials, subjects, and conditions

performance of CWLs for correct trials (Dimitriadis et al., 2015b).

To assess the statistical significance level of *PLV* estimates, we used the Rayleigh test for the uniformity of *PLV* values as previously described (Dimitriadis et al., 2013, 2015a,b,c,d, 2016a,b; for further details see Supplementary Material Section 2B).

Effective Connectivity and Time Delay between F^{θ} and $PO^{\alpha 2}$

Dynamic causal modeling, structural equation modeling, and granger causality

Effective connectivity is defined as "the influence one system exerts over another" (Friston, 2011). It is important to mention that functional connectivity is not necessarily effective connectivity. Only effective connections are directed from one brain area to another. Many techniques have been proposed to explain causal interactions in multichannel neuroimaging recordings, including like dynamic causal modeling (DCM), structural equation modeling (SEM), and Granger causality (GC).

GC is a statistical concept of causality that predicts the future of an activity X based on the past activity Y. Two time series {X,Y} (e.g., EEG/MEG/fMRI oscillations) have a causal relationship when past values of X can be useful for predicting future values of Y. This terminology of causality was first formulated by Granger (1969). In the last 10 years, GC has gained much attention in the neuroscience community (Kaminski et al., 2001; Barnett and Seth, 2014).

The main goal of DCM in neuroimaging data based on a set of regions of interest (ROIs) is to determine the causal influence of each ROI on the others and study the experimental influence on the connections' strengths. The aforementioned procedure demands: (i) biophysically and physiologically plausible models of neuronal network dynamics that can predict the pattern of the network topology that better described the connectivity of a spatially distinct predefined subset of ROIs related to the experimental stimuli and (ii) efficient and computationally feasible statistical parametric estimations and model comparisons that better fit the experimental data, leading to meaningful directed networks that are supported by the literature (Friston et al., 2003). DCM is a Bayesian model comparison procedure between candidate models that better describes experimental data. Dynamic causal models are described via ordinary differential equations that are non-linear state-space models. These equation-based models describe the dynamics of hidden states in a set of nodes of a probabilistic graphical model where their conditional dependencies are parameterized via directed effective connectivity. The probabilistic graphs in DCM can be cyclic (the estimated graphs cannot be cyclic in GC or SEM), and DCM does not assume that random fluctuations are uncorrelated (Downey and Hirschfeldt, 2010), unlike GC and SEM.

The aim of DCM is to infer the causal architecture of coupled or distributed dynamical systems. This Bayesian model comparison procedure rests on comparing models of how data were generated. Dynamic causal models are formulated in terms of stochastic or ordinary differential equations (i.e., non-linear state-space models in continuous time). These equations model the dynamics of hidden states in the nodes of a probabilistic graphical model, where conditional dependencies are parameterized in terms of directed effective connectivity. Unlike Bayesian networks, the graphs used in DCM can be cyclic, and unlike SEM and GCM, DCM does not depend on the theory of algorithmic randomness (Downey and Hirschfeldt, 2010).

In fMRI, DCMs typically rely on two classes of states, namely "neuronal" and "hemodynamic" states. The latter encodes neurovascular coupling for modeling fMRI signal variance generated by neural activity (Friston et al., 2003). Biophysical models in DCMs for EEG/magnetoencephalography (MEG)/LFP data are typically more complex than in DCMs for fMRI. This is because the richness in temporal information contained by electrophysiologically measured neuronal activity can only be recorded by neurobiological models. The report introducing DCM for EEG/MEG data (David et al., 2006) relied on a so-called "neural mass" model.

Following the initial paper by David et al. (2006), a number of extensions to this "neural mass model"-based DCM were proposed that considered both spatial and temporal aspects of MEG/EEG data. Concerning the spatial domain, one problem is that the position and extent of cortical sources are difficult to precisely specify *a priori*. Kiebel et al. (2006) proposed to estimate the positions and orientations φ of "equivalent current dipoles." Concerning the temporal domain, computational problems can arise when dealing with recordings of enduring brain responses where it is more efficient to summarize the measured time series in terms of their spectral profile. This is the approach developed by Moran et al. (2007, 2008, 2009), which models LFP data based on the neural mass model using a linearization of the evolution function f around its steady state (Moran et al., 2007).

Structural equation modeling analyses start with a set of ROIs and try to estimate the connection strengths between the predefined ROIs leading to a model that best describes the connectivity pattern. The connections in the model are directional and represent the degree of correlation between the time series describing ROI activities. SEM procedures can vary, but most of them are based on general linear modeling (GLM) searching through the space of possible sets of connections that best fit the data (Graham, 2008). A comparison between dynamic (DCM) and static (SEM) effective connectivity analyses was published by Penny et al. (2004a,b).

For a better understanding of the various techniques of DCM, SEM and GC, an interested reader should refer to the original papers, the main extensions of the techniques and to well-presented reviews (Daunizeau et al., 2011; Friston, 2011; McIntosh and Mišić, 2013).

Causal interactions and time delay between F^{θ} and $PO^{\alpha 2}$

To unfold both causal interactions and the time delay between F^{θ} and $PO^{\alpha 2}$, we adopted the dSTE method (Dimitriadis et al., 2016a). Compared to GC (Granger, 1969), the adopted technique of STE is a model-free approach of effective connectivity that is not affected by outliers or filtering and can be directly applied to non-stationary multichannel recordings. This is in comparison to GC that assumes only stationary signals and is

affected by various filtering options (for a comparison study see Papana et al., 2013). Partial direct coherence (PDC) and direct transfer function (DTF) are the best options when we analyze time series from linear systems that operate on the same frequency. In our case, we proposed for the first time a causality estimator called dSTE for time series with different frequencies that can detect the strength, direction and lag between non-linear and non-stationary multichannel recordings (Dimitriadis et al., 2016a; see Supplementary Material Section 3).

To strengthen our hypothesis that activity in frontal brain regions precedes parietal activity in cognitive control (Brass et al., 2005), we adopted a new technique that addresses the time lag between two time-series based on cross-correlation of instantaneous amplitudes of two oscillations (Adhikari et al., 2010) (see Supplementary Material Section 4). The technique was adopted supplementary to the time-lag detection based on our target method (see Supplementary Material Section 3).

Uncovering Causal Phase Relationship between F^{θ} and $PO^{\alpha 2}$

We detected and quantified the strength of causal phase interactions between F^{θ} and $PO^{\alpha 2}$ brain areas via the dPLI (Stam and van Straaten, 2012). The dPLI obtains the phase difference between two time series (A and B) based on the following formula:

$$dPLI = \frac{1}{N}\sum_{t=1}^{N} H\left(f\left(t\right)\right) \tag{3}$$

There are three cases based upon the distribution of the phase difference within $[-\pi, \pi]$:

(a) Most of the phase differences between two time series are in the interval of $0 \leq \Phi(t) \leq \pi$, and signal A is consistently leading in phase domain signal B with a $dPLI > 0.5$
(b) Phase difference of the two signal are on average π radians out of phase where we cannot say anything about who drives who
(c) Most of the phase differences between two time series are in the interval of $\pi \leq \Phi(t) < 0$, and signal B is consistently leading in phase domain signal A with a $dPLI < 0.5$

After applying the proper statistical filtering approach (see Supplementary Material Section 5), we aggregated the strength of the significant causal relationship between F^{θ} and $PO^{\alpha 2}$ brain sites.

PAC between F^{θ} and $PO^{\alpha 2}$

Cross-frequency interactions between F^{θ} and $PO^{\alpha 2}$ were also assessed via PAC. The algorithm was adopted to our EEG multichannel recordings as described below. Let $x(i, t)$ be the EEG activity recorded at the ith site, $x(j, t)$ be the EEG activity recorded at the jth site, and $t = 1, 2, \ldots, T$, represents the successive time points. Given two frequency band-limited signals $x(i, t)$ and $x(j, t)$, cross-frequency coupling and namely PAC directly estimated the strength of the phase of the low-frequency (LF) oscillations to modulate high-frequency (HF) oscillation amplitude. The complex analytic representations of both signals $Z_{LF}(t)$ and $Z_{HF}(t)$ are extracted via the Hilbert transfer (HT):

$$\begin{aligned} Z_{LF}(t) &= HT\left[X_{LF}(t)\right] = Z_{LF}\, e^{i\phi_{LF}(t)} = A_{LF}(t)\, e^{i\phi_{LF}(t)} \\ Z_{HF}(t) &= HT\left[X_{HF}(t)\right] = Z_{HF}\, e^{i\phi_{HF}(t)} = A_{HF}(t)^{i\phi_{HF}(t)} \end{aligned} \tag{4}$$

Then, the envelope of the HF oscillations, $A_{HF}(t)$ is filtered within the range of LF oscillations (here in θ) and from the filtered signal, phase dynamics $\varphi'(t)$ are derived via an HT:

$$Z'(t) = HT\left[A_{HF,LF}(t)\right] = \left|Z'(t)\right| e^{i\phi'_{HF}(t)} = Z'(t)^{i\phi_{LF\rightarrow HF}(t)} \tag{5}$$

The aforementioned formula describes the modulation of the amplitude of HF-oscillations by the phase of LF-oscillations and adopting *PLV* (Eq. 1) as an index of the PAC strength, we can quantify the phase consistency of these two time series. Again, we aggregated the strength of significant PAC estimates between F^{θ} and $PO^{\alpha 2}$ (Dimitriadis et al., 2015a, 2016a; see Supplementary Material Section 6).

Accessing Classification Performance between Correct and Wrong Trials

We commence this subsection by including the classification strategy using a set of features including signal characteristics, behavioral data, PS, phase coupling, and dSTE. The total number of wrong trials within the group was 277 and distributed in each CWL as followed: $Lv1 = 42$, $Lv2 = 53$, $Lv3 = 59$, $Lv4 = 62$, and $Lv5 = 61$ (Lv = level of difficulty). Since the individual total number of wrong trials across CWL ranged from 1 to 13, we trained the binary classifier by manipulating correct and wrong trials from the whole group. The above procedure will strengthen our results by presenting the classification performance with a group-unified classifier. The classification scheme was based on PS, phase coupling within F and PO brain areas on their prominent frequency (θ in F and α_2 in PO), cross-frequency phase-to-phase coupling between F^{θ} and $PO^{\alpha 2}$, PAC between the phase of F^{θ} and the amplitude of $PO^{\alpha 2}$, directed cross-frequency amplitude-to-amplitude coupling based on dPLI between F^{θ} and $PO^{\alpha 2}$, and dSTE between F^{θ} and $PO^{\alpha 2}$. This scheme was followed for each CWL independently between correct and wrong trials (binary classification).

For PS and reaction time measurements, we employed the Laplacian score as a feature extraction technique (He et al., 2005), and a k-NN classifier served as the predictor of correct versus wrong trials for each CWL. In the feature-extraction step, signal-power was separately estimated from the selected EEG sensors for each single-trial segment for θ band P^{θ}, α_2 band $P^{\alpha 2}$, and the corresponding ratio $P^{\theta}/P^{\alpha 2}$ in both PO and F brain areas. We augmented this large number of features with the reaction time. We further normalized all features within the [0, 1] range. Complementary to PS and reaction times, we classified correct versus wrong trials based on the different representations of FCGs estimated with a large repertoire of connectivity estimators. For the classification strategy, we adopted a previously published approach based

on the tensorial treatment of FCGs (Dimitriadis et al., 2013, 2015d,c; Antonakakis et al., 2016). We adopted a 10-fold cross-validation scheme for both signal-power/reaction time and different functional connectivity representations (see Supplementary Material Section 7).

RESULTS

Behavioral Results

We first compared response times and subject performance between consecutive CWLs. Adopting Wilcoxon rank-sum tests and Bonferroni corrections, we revealed the expected effect of difficulty for response time ($p < 0.001$, Bonferroni corrected, $p' < p/4$) with longer responses to be linked to higher CWLs and higher difficulty. In terms of accuracy, we demonstrated a decreasing trend across the increment of difficulty, but it was not significant after correcting for multiple comparisons (for $p < 0.001$, Bonferroni corrected, $p' < p/4$) (see Supplementary Material Section 8). Additionally, no statistical differences were detected between correct and wrong trials based on response times (**Figure 2**).

Power Spectrum Evidence in F^{θ} and $PO^{\alpha 2}$ Related with Arithmetic Performance

We performed Wilcoxon rank-sum tests to find significant differences between correct and wrong responses in terms of the PS (see Supplementary Material Section 1). Our analysis did not reveal any significant tendency of the PS in F^{θ} and $PO^{\alpha 2}$ regarding the behavioral response (correct *vs.* wrong trials). Interestingly, we found significant increasing trends for both F^{θ} and $PO^{\alpha 2}$ following task difficulty in both correct and wrong trials (**Figure 3**).

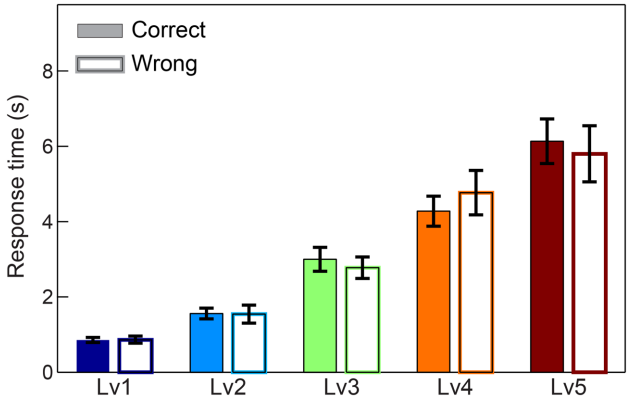

FIGURE 2 | Response times across five CWL in both correct and wrong trials. Bars represent mean ± standard error of mean (SEM). No significant difference was observed in the response time between correct and wrong trails.

Intra- and Inter-frequency Phase Coupling within and between WM Subsystems

Any significant difference between correct and wrong responses in terms of strength related to different types of phase interactions was analyzed via Wilcoxon rank-sum testing. The subgraph strength for either F or PO brain regions was the total weight of all the connections within each of the brain areas and was estimated for each subject by averaging across trials and for each CWL. We found that the five different types of phase memory synchronization showed a decrement tendency with the increment of the CWL in both correct and wrong trials. However, our analysis failed to reveal any significant difference between correct and wrong responses. Phase interactions within F^{θ} (**Figure 4A**) and $PO^{\alpha 2}$ (**Figure 4D**), n:m (2:1) θ-α_2 phase interactions between F^{θ} and $PO^{\alpha 2}$ (**Figure 4C**), within $F^{\theta-\alpha 2}$ (**Figure 4B**), and within $PO^{\theta-\alpha 2}$ brain regions (**Figure 4E**) did not show any significant effect related to arithmetic performance (**Figure 4**).

Strength of Phase Causal Interactions and Phase-to-Amplitude Interactions

The significance level of the strength related to dPLI and PAC was assessed with Wilcoxon rank-sum testing. Our analysis failed to reveal any significant difference between correct and wrong responses for both types of brain synchronization (**Figure 5**). Additionally, dPLI did not demonstrate any effect of task difficulty, whereas PAC strength diminished with greater difficulty for both correct and wrong trials.

Causal Interactions and Time-Lag between WM Subsystems

Before applying statistical tests to causal interactions between correct and wrong answers, we adopted a two-step averaging procedure: (i) averaging across trials for each subject independently and (ii) averaging across subjects. Our statistical analysis was based on Wilcoxon rank-sum tests ($p < 0.001$). To correct for multiple testing, we adopted the false discovery rate (FDR) method to correct for multiple testing and applied it to each trial (Benjamini and Hochberg, 1995). Adopting dSTE to estimate causal interactions between F^{θ} and $PO^{\alpha 2}$, we found a significant trend: F^{θ} drives $PO^{\alpha 2}$ (**Figure 6**). The statistical analysis uncovered F^{θ}-$PO^{\alpha 2}$ dysfunction in wrong trials to each CWL compared to correct trials (**Figure 6**). **Figure 6** shows the significant interactions. Both dSTE and cross-correlation of amplitude envelopes between F^{θ} and $PO^{\alpha 2}$ show that F activity precedes that of PO in both correct and wrong trials. Importantly, time-lag estimation with both dSTE and cross-correlation of amplitude envelopes revealed an interesting trend in wrong trials compared to correct: right PO ($rPO^{\alpha 2}$) brain region (i.e., channels P6, P8, PO8, PO4, and O2) showed zero time-lag with bilateral F brain regions (bF^{θ}) across the five CWLs (**Figure 7**). **Table 1** summarizes the group-average time-lag (in ms) between bF^{θ} and $rPO^{\alpha}{}_2$ estimated with $dSTE^{NG}$ for each CWL based on correct trials.

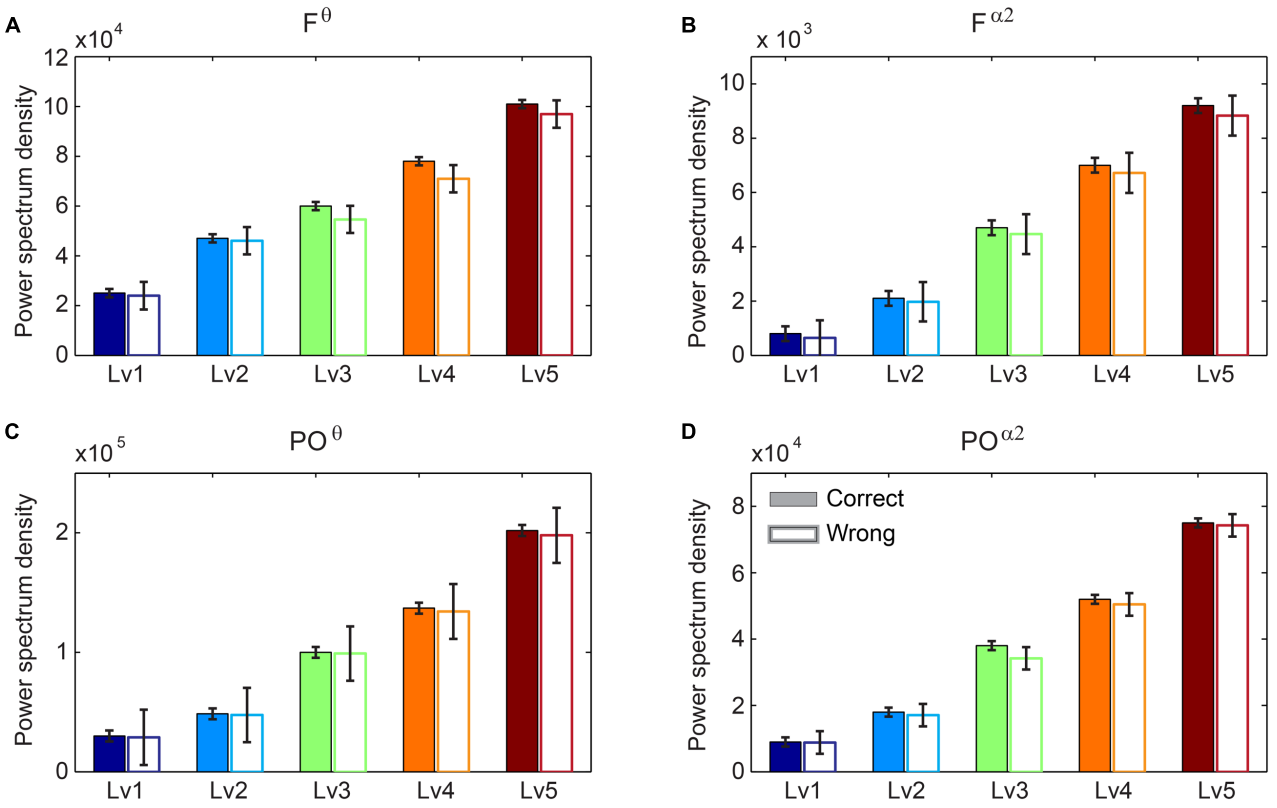

FIGURE 3 | Group-averaged power spectrum in θ band (5–6 Hz) (A) over frontal (F) bilaterally areas and (C) over parieto-occipital (PO) sites and in α2 band (10–13 Hz) (B) over F bilaterally areas and (D) over PO sites for the five CWLs in both correct and wrong trials. Bars represent mean ± standard error of mean (SEM). No statistical significant differences were detected based on Wilcoxon rank sum test ($p < 0.001$; Bonferroni corrected across CWLs).

Classification Performance based on Behavioral, Power Spectrum, and Connectivity Analysis

The classification performance, based on PS expressed via a group-averaged correct recognition rate, was 58.8 ± 11.2% (**Table 2**). The Laplacian score only detected the PS as a useful feature to improve the binary classification of correct versus wrong trials at each CWL (see Supplementary Material Section 7). The classification performance based on PS was marginally at by chance classification performance (50%). We present the results based on functional connectivity estimates following alternative strategies with the goal of differentiating correct from wrong trials for each CWL using the single-trial subgraph connectivity estimates from all subjects. The group-averaged performance of the tensor subspace analysis + k-nearest neighbor classifier (TSA + k-NN) scheme based on F^{θ}, $PO^{\alpha 2}$, and the CFC was 65.0 ± 12.1% (**Table 2**). When we applied the TSA + k-NN strategy to the F^{θ} and $PO^{\alpha 2}$ subgraphs, the classification performances were 61.1 ± 8.4% for θ and 56.5 ± 8.1% for α_2, (**Table 2**) (for further details see Supplementary Material Section 7). We further analyzed correct and wrong trials based on cross-frequency phase-to-phase coupling between F^{θ} and $PO^{\alpha}{}_2$ where the maximum classification performance was held on for the fifth CWL reaching 65.1 ± 12.1%. Phase-to-amplitude coupling between F^{θ} and $PO^{\alpha}{}_2$ improved the classification accuracy of phase-to-phase coupling, but this was not significant and reached 68.35 ± 9.3% in the fifth CWL. Cross-frequency coupling was also analyzed via the directionality of the amplitude-to-amplitude activity in F^{θ} and $PO^{\alpha}{}_2$ using dPLI and the novel dSTE using the tensorial approach for comparable purposes with the previous connectivity estimators. Based on the strength, effective connectivity graphs that incorporated dPLI showed the highest score for the fifth CWL at 69.4 ± 13.5%. In contrast, effective connectivity graphs that incorporated the strength of dSTE between F^{θ} and $PO^{\alpha}{}_2$ (**Figure 7**) revealed a group-averaged performance of the TSA + k-NN scheme equals to 100% (**Table 2**). Additionally, we previously stated that $rPO^{\alpha 2}$ showed a zero time-lag with bF^{θ} across the five CWLs in the wrong but not correct trials (**Figure 7**).

DISCUSSION

Two recent dual recording studies (EEG and LFP) uncovered the different roles of amplitude and phase in brain activity (Ng et al., 2013; Musall et al., 2014). Many neuroimaging studies have demonstrated the different functional roles of WM subsystems in various cognitive tasks. EEG WM rhythms such as θ and α are

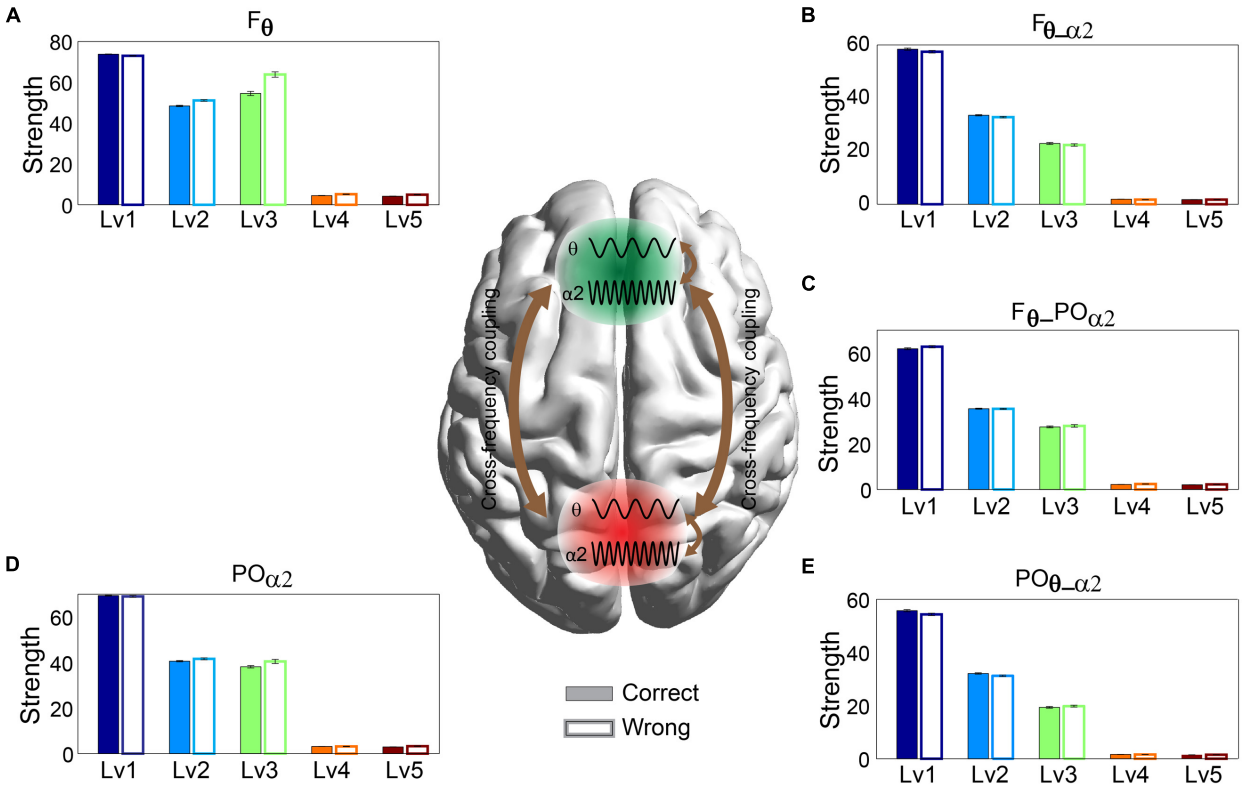

FIGURE 4 | Strength distribution of within- and between-phase interactions located over F brain regions: (A) within-phase interaction in Frontal (F^{θ}), (B) between-phase interaction in Frontal ($F^{\theta-\alpha 2}$), (D) within-phase interaction in Parieto-Occipital ($PO^{\alpha 2}$), and (E) between-phase interaction in Parieto-Occipital ($PO^{\theta-\alpha 2}$) and (C) cross-frequency coupling between them ($F^{2\ \times\ \theta}$ – $PO^{\alpha 2}$) for both correct and wrong answers. Bars represent mean ± standard deviations. No statistical significant differences were detected between correct and wrong trials.

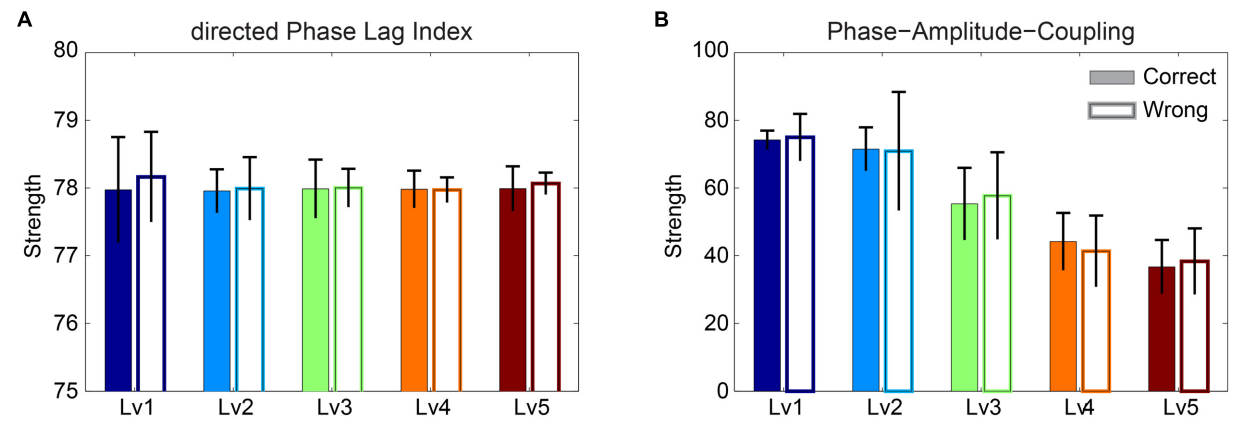

FIGURE 5 | Strength of (A) dPLI and (B) PAC between Frontal$^{\theta}$ and Parieto-Occipital$^{\alpha 2}$ ($F^{2\ \times\ \theta}$ – $PO^{\alpha 2}$) for both correct and wrong answers. Bars represent mean ± standard deviations. No statistical significant differences were detected between correct and wrong trials.

located in the well-defined F and PO brain regions, respectively (Kawasaki et al., 2010). A WM study based on modeling demonstrated that input information is stored in posterior brain areas by α rhythm (Chik, 2013), while short-term-stored representations are manipulated within the frontal executive WM systems by the θ rhythm, which also connects frontal and posterior brain sites (Kane and Engle, 2002). In the present study, we attempted to demonstrate how the central executive and storage buffer WM subsystems operate during an arithmetic task and also how their coordination affects arithmetic performance. We assessed the functionality of both WM subsystems oscillating in the preferred phase with PS analysis, intra-/inter-frequency

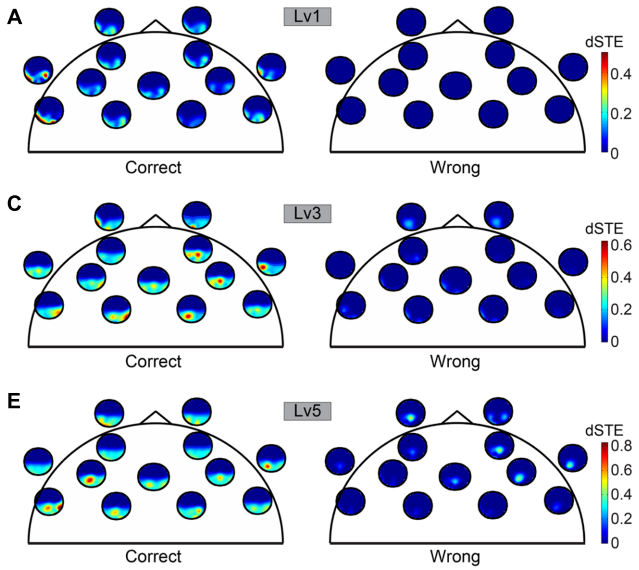

FIGURE 6 | To represent dSTE for each of the five cognitive workload levels [(A) Lv1, (B) Lv2, (C) Lv3, (D) Lv4, and (E) Lv5] and in both correct (left panel) and wrong trials (right panel), we adopted a novel visualization scheme, in which the relative position of a single sensor u is used to embed a whole brain's topography that represents the dSTE(u,v) measurements related to it. A minute topography depicts the dSTEs from a particular sensor to all other destinations (sensor locations). It serves as a natural display of a row in the dSTE matrix. The topographic representation illustrates only the Frontal sensors because ΔdSTE uncovered F^{θ} brain region as a leader.

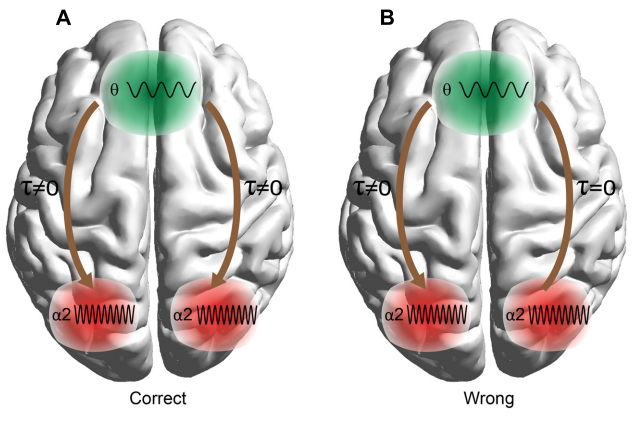

FIGURE 7 | Time-lag effects between F and PO sites in (A) correct and (B) wrong trials. The analysis detected time-lag effects for three out of four combinations (right and left PO × correct and wrong trials) with the exception of bilateral F and right Parieto-Occipital sites in wrong trials.

phase coupling (Palva et al., 2005; Kawasaki et al., 2010; Palva and Palva, 2012; Dimitriadis et al., 2015b,a), and causal interactions between different frequencies on both amplitude (Dimitriadis et al., 2016a) and phase (Stam and van Straaten, 2012).

The current study aimed to shed light on the mechanisms and EEG features that contribute to correct behavioral performance. To validate our analysis, we used PS and different types of connectivity estimators based on amplitude, phase, and their causal interactions between F and PO brain areas. Apart from identifying the best feature that can predict behavioral performance in the mental arithmetic task, we wanted to highlight the potential to link performance in a difficult cognitive task with an individual's brain activity. Our approach could be used as a framework for alternative complex tasks using either EEG or MEG imaging methods. Additionally, the entire methodology can be employed to design an appropriate intervention for dyscalculic subjects who face problems with numeric calculations by focusing on specific attributes of brain dynamics.

Our main results can be summarized in the following four summary points:

- With regard to the level of oscillatory amplitudes in both WM brain regions, the current study did not identify significant differences between correct and wrong responses in terms the PS estimated on both θ and α_2 frequencies over F and PO brain regions as an integrated estimator. Additionally, reaction times did not reach a statistically significant level between correct and wrong trials.
- Our connectivity analysis focused on various interaction types within and between the WM subsystems oscillating on the prominent frequencies. We adopted intra- and inter-frequency estimators to uncover causal effects between the different frequencies extracting both the time-lag and coupling strength. The adopted estimators were amplitude and phase-oriented as follows: *n*:*m* phase locking estimator (inter-frequency coupling based on phase), dPLI (inter-frequency coupling based on amplitude), PAC (inter-frequency estimator between the phases and amplitudes of two different frequencies), and *PLV* (intra-frequency coupling) failed to discriminate correct from wrong trials for each CWL.

- By employing dSTE to estimate causal interactions (both strength and direction) between F$^{\theta}$ and PO$^{\alpha}{}_2$, we successfully classified 100% of correct from wrong trials for each subject independently.
- Both dSTE and cross-correlation of amplitude envelopes revealed that F$^{\theta}$ drives PO$^{\alpha 2}$ in both correct and wrong trials with the only exception of bilateral F (bF$^{\theta}$) and right PO (rPO$^{\alpha}{}_2$) sites in wrong trials (**Figure 7**).

Frontal Midline θ Implication to Mental Arithmetic

Generators of frontal midline θ are located on the dorsal part of the anterior cingulate cortex (ACC) and the adjacent medial PFC; both structures are related to focused attention and many cognitive functions associated with mental calculation (Ishihara and Yoshi, 1972; Sasaki et al., 1996; Asada et al., 1999; Enriquez-Geppert et al., 2014). The ACC encompasses various emotional, cognitive, executive, and visuospatial functions (Bush et al., 2000; Womelsdorf et al., 2010). A recent study based on continuous subtraction noted a significant increment of θ power within the ACC (Ishii et al., 2014). Additionally, the dorsal ACC is part of the distributed attentional brain network (Bush et al., 2000). Our results clearly demonstrate a statistically significant increment of power in F$^{\theta}$ over task difficulty but no statistically significant difference between correct and wrong trials (**Figure 3**).

WM and Mental Tasks

WM tasks like mental calculations require distinct functions such as a storage buffer, central executive functions, and coordination between them. The posterior brain regions play a general role in maintaining actual contents of representations (Todd and Marois, 2004; Vogel and Machizawa, 2004). Previous studies also revealed an attentional control role for the PFC; it is responsible for determining which information will be maintained and updated within the WM but is not involved in the maintenance of the relevant information (Cohen et al., 1997; Smith and Jonides, 1999; Rowe et al., 2000; Kawasaki et al., 2006). Other neuroimaging studies hypothesized that WM processes are controlled via top-down signals from the PFC to the posterior brain areas where the mental representation of the related information is stored (Baddeley, 1992; Miller and Cohen, 2001; Curtis and D'Esposito, 2003). A typical mental arithmetic study involved a task-activated distributed network of brain areas including the frontal cortex and bilateral parietal lobes (Dehaene et al., 2004; Pinel et al., 2004).

WM and selective attention have been extensively viewed as separate cognitive domains. In contrast, a growing number of theoretical assessments and reviews in the fields of neuroscience and psychology have reported that these two domains share commonalities (Awh et al., 2006; Postle, 2006; Chun, 2011). Research primate and human neuroimaging studies have already shed light on the significant role of top-down signaling to enhance brain activity in areas related to the stimuli modality while simultaneously suppressing brain activity for distracted stimuli to the targeted goals. Specifically in visual areas, changes related to excitation levels reflected a simultaneous competitive substrate for items represented in receptive fields and a synchronized pattern of neural ensembles (Reynolds and Chelazzi, 2004). The neuroscience community supports the hypothesis that top-down modulation of external sensory information relies on distant interactions (e.g., between the PFC and parietal cortex) and not an intrinsic functionality of modality-specific sensory cortices (Curtis and D'Esposito, 2003; Gazzaley and D'Esposito, 2007). In a delayed recognition task, Zanto et al. (2011) demonstrated that Frontal-Parietal α band (7–14 Hz) phase coherence served as the substrate for long-distance, top-down modulation and provided clear evidence that top-down modulation mediated by the PFC causally links early attentional processes and subsequent memory performance.

Prominent WM Frequencies of Frontal and Parietal Brain Regions

It is well known that posterior brain areas maintain information related to the modality while the frontal cortex actively manipulates associated information (Postle et al., 1999; Smith and Jonides, 1999; Curtis and D'Esposito, 2003; Wager and Smith,

TABLE 1 | Group-average time-lag (mean ± SD) between bF$^{\theta}$ and rPO$^{\alpha 2}$ estimated with dSTE^{NG} for each cognitive workload level (CWL) based on correct trials.

Workload level	Lv1	Lv2	Lv3	Lv4	Lv5
Time-lag (ms)	117 ± 14	121 ± 17	114 ± 21	132 ± 14	133 ± 17

TABLE 2 | Classification behavioral performance based on power spectrum (PS), phase coupling (PC), phase-to-amplitude cross-frequency coupling (CFC), causal phase relationships directed phase lag index (dPLI) and delay symbolic transfer entropy (dSTE).

	Lv1	Lv2	Lv3	Lv4	Lv5
PS	57.1 ± 13.2%	53.1 ± 10.2%	56.2 ± 9.2%	58.8 ± 11.2%	58.1 ± 9.8%
PC$^{\theta}$	55.6 ± 10.1%	56.2 ± 8.7%	61.1 ± 8.4%	54.3 ± 7.8%	57.3 ± 10.2%
PC$^{\alpha 2}$	54.3 ± 8.2%	56.3 ± 12.3	55.3 ± 6.5%	56.5 ± 8.1%	53.4 ± 7.3%
PC^{CFC}	58.4 ± 7.4%	59.3 ± 9.1%	58.9 ± 12.3%	60.1 ± 10.1%	65.1 ± 12.1%
PAC^{CFC}	60.2 ± 9.2%	61.7 ± 8.7%	64.4 ± 10.7%	63.3 ± 9.4%	68.4 ± 9.3%
dPLI^{CFC}	61.8 ± 10.1%	65.2 ± 11.3%	65.7 ± 9.5%	65.8 ± 12.5%	69.4 ± 13.5%
dSTE	100%	100%	100%	100%	100%

2003). An increment of θ activity within frontal brain areas is an indicator for increased cognitive demand and focused attention (Yamada, 1998) while decrement of upper α is an index of distinct functions related to task processing (Klimesch, 1999). Even though our experimental paradigm was not designed with a clear discrimination of the manipulation and retention periods, various studies have established the roles of both frequencies and WM brain areas in mnemonic processes (Micheloyannis et al., 2005; Palva et al., 2005; Fell and Axmacher, 2011; Palva and Palva, 2012). Our results based on signal power and brain connectivity with both intra- and inter-frequency phase-to-phase coupling further support the distinct role of both oscillations θ for manipulation and α_2 for maintenance, as dominant frequency rhythms in WM subsystems in F and PO, respectively. Additionally, the retention period of the adopted experimental paradigm apart from representation maintenance support other distinct functions like preparation and task-related rule maintenance. Previous EEG studies demonstrated phase synchronization between θ and α_2 brain rhythms in many brain areas in a high number of WM tasks (Jensen and Tesche, 2002; Mizuhara et al., 2004; Sauseng et al., 2005; Kawasaki and Watanabe, 2007; Klimesch et al., 2008).

Interplay between Frontal and Parietal Brain Regions

Although many neuroimaging studies suggest that PFC plays a key role in the cognitive control, interplay between the PFC and parietal cortex was emphasized (Brass et al., 2005). This raises a fundamental question about the different contributions of these brain areas in cognitive control. It was assumed that the PFC biases processing in posterior brain regions (Miller and Cohen, 2001; Brass et al., 2005). This assumption led to the hypothesis that neural activity in the PFC should precede parietal activity in cognitive control (Brass et al., 2005). Our study uncovered a causality effect between F^{θ} and $PO^{\alpha 2}$ brain regions in the five CWLs (**Figure 6**). The PFC serves to add bias signals to other brain structures (e.g., the parietal cortex) to guide stimulus and response processing toward the desired behavior (Miller and Cohen, 2001; Brass et al., 2005). Additionally, a zero time-lag between rPO^{a2} and bF^{θ} brain regions was detected in wrong trials and across the five CWLs (**Figure 7**). A possible explanation of the above significant observation could be attributed to the arithmetic nature of the task and particularly to right posterior parietal cortex oscillation in the preferred α_2 frequency in which both frequency and brain region are integrated for semantic understanding (Sauseng et al., 2005; Klimesch et al., 2008) and spatial representation of numbers (e.g., a mental number line Hubbard et al., 2005, 2009; Gobel et al., 2006).

Involvement of Parietal Brain Areas in Math Calculations

Based on findings from previous studies, the intraparietal sulcus is a systematically activated brain area during number manipulation independently of their notation (i.e., digits, dots, plurals of nouns; Carreiras et al., 2015). For this reason, the intraparietal sulcus is activated in all arithmetic tasks as the neural substrate for manipulating quantities or numbers (Dehaene et al., 2003, 2004; Kong et al., 2005). Both subtraction and addition elicit higher intraparietal sulcus activation compared to other arithmetic tasks like multiplication and division. Compared to multiplication where part of the results are stored in rote verbal memory, the addition of numbers is not learned by rote and demands quantity manipulation (Dehaene et al., 2003, 2004). Inferior and postero-superior parietal lobules have been linked to both counting and subtraction (Dehaene et al., 2003). Compared to the intraparietal sulcus that is mainly activated by number representations, the postero-superior parietal area plays a key role in numerous visuospatial tasks that demand attention with or without WM activation (Mitchell and Cusack, 2008; Olson and Berryhill, 2009). The aforementioned findings suggest that postero-superior parietal cortex activation is related to processing attended stimuli. For that reason, the well-known mental number line, a quasi-spatial representation of numbers organized on their proximity, can be the core semantic abstract representation of numerical quantities. It was clearly demonstrated that the process followed in covert attention that is activated to select target locations in space can also be engaged when numbers in arithmetic tasks are manipulated independently of the notation over the mental number line located in the parietal cortex (Dehaene et al., 2004). The PSP lobule is involved in this spatial-attention hypothesis in both visuospatial tasks where the information is presented and in non-visual arithmetic tasks (Ishii et al., 2014).

Untangling Arithmetic Performance via the Causal Relationship

To summarize, our findings based on causal interactions of the θ and α_2 rhythms demonstrate the need for communication between frontal and parietal WM subsystems for better mental arithmetic paradigm outcomes (Fell and Axmacher, 2011). The strength of the causality between F^{θ} and $PO^{\alpha 2}$ in correct trials and the zero time-lag between bF^{θ} and $rPO^{\alpha 2}$ in wrong trials explain arithmetic performance in the five CWLs and unmask the executive role of the PFC in cognition (Miller and Cohen, 2001; Brass et al., 2005). Additionally, the zero time-lag between $rPO^{\alpha 2}$ and bF^{θ} in wrong trials improve understanding of the hierarchical spatiotemporal functionality of brain rhythms underlying cognition (Furl et al., 2013). A scalp-EEG brain connectivity study that employed a WM task revealed the need for connectivity between F^{θ} and $PO^{\alpha}{}_2$ activity, supporting the need of hierarchical control between F and PO in many spatiotemporal domains and for various cognitive processes like WM (Kawasaki et al., 2010). Finally, in primates, the PFC exerts executive control over cognition by transmitting signals to parietal brain regions in a rule-based spatial categorization task (Crowe et al., 2013). Studies of lesion subjects revealed clear involvement of the right parietal cortex in mental arithmetic processing. Dehaene and Cohen (1997) presented the first report based on two acalculic subjects with structural lesions affecting the right parietal cortex or left subcortical areas. They demonstrated that the subject

with a left structural lesion had impaired rote arithmetic facts that were analyzed based on *a priori* knowledge of numerical quantities. However, the patient with a right inferior parietal lesion exhibited significant impairment of quantitative numerical knowledge, which was more severe for subtraction tasks (Dehaene and Cohen, 1997). In addition, a recent study of cortical electrostimulation in patients with brain tumors confirmed an anatomico-functional organization for arithmetic processing within the right parietal cortex (Della Puppa et al., 2013).

In general, neuronal oscillations at different frequencies were recently connected with basic higher cognitive processes, further supporting the distinct functional role of each brain rhythm during WM [for a review, see (Roux and Uhlhaas, 2014)]. The α brain rhythm expresses the level of inhibition of task-irrelevant activity, while θ rhythm supports the temporal organization of abstract items in the WM (e.g., the intermediate results from the addition tasks in the present study). Pairs of cross-frequency couplings like α-γ and θ-γ have a distinct role in managing WM information [for a review, see (Roux and Uhlhaas, 2014].

Top-down manipulation of processing of sensory information is supported by distant interactions like between the PFC and parietal cortex (Curtis and D'Esposito, 2003; Miller and D'Esposito, 2005; Gazzaley and D'Esposito, 2007) and on interactions within these two subnetworks. Zanto et al. (2011) demonstrated that Frontal-Parietal α band (7–14 Hz) phase-coherence is the substrate for distant top-down modulation via the PFC to other activated distributed brain areas and links attentional processes and related memory performance. Summarizing existing evidence in terms of the distinct role of each frequency in WM tasks, the causal role of the PFC over parietal brain areas, right parietal involvement in quantitative numerical knowledge, and our findings, we can untangle the significant prediction of arithmetic performance. The loss of top-down control of the PFC over the right PO area can be interpreted as an interruption between these two brain areas and the major role of the PFC in overall cognitive control (Brass et al., 2005). A possible explanation of the above significant observation is the arithmetic nature of the task; particularly, the right posterior parietal cortex oscillates in the preferred α_2 frequency, so both frequency and brain region are integrated for semantic understanding (Sauseng et al., 2005; Klimesch et al., 2008), spatial number representation (similar to a mental number line; Hubbard et al., 2005, 2009), and the loss of inhibition of task-irrelevant activity.

Top-down modulation supports our ability to pay attention to task-relevant stimuli and suppress irrelevant distracted information. The common prediction of arithmetic performance across subjects and in the five CWLs was the inability of the subject to inhibit irrelevant distracted information; they then lost the ability to give a correct answer even on the first levels with simple addition. The current findings are among the first cognitive neuroscience results that adopted a large repertoire of connectivity estimators and succeeded in clarifying the distinct role of each frequency distributed over specific anatomical brain areas, each with a different role in WM arithmetic mental tasks. Finally, our findings will be useful for studying mental arithmetic tasks in aging adults and dyscalculic children, as well as guiding neurofeedback strategies.

Limitations

One of the major limitations of the present study is that the sensor space connectivity analysis lacks the higher spatial resolution that would be achieved by performing the same analysis in the source space. Despite tremendous improvements in MEG and EEG source localization algorithms, one should compare the connectivity analysis between sensor and space to be aware of the spatial filtering effect. Field spread effect can never be totally diminished or abolished after applying a source localization technique (Schoffelen and Gross, 2009); however, applying source connectivity will further enhance both the results of the present study and the interpretation of active areas related to the tasks by taking the advantage of a larger number of fMRI arithmetic studies.

CONCLUSION

In the present study, we attempted to provide the first demonstration of dynamic orchestration between θ oscillations and modality-specific high α_2 oscillations as the link between central executive system (F^{θ}) and storage buffer functions ($PO^{\alpha}{}_2$) in a WM-oriented multilevel mental task. Our analysis focused on the comparison between correct and wrong answers to reveal significant differences between and within WM subsystems. To uncover the distinct roles of amplitude and phase under the notion of connectivity, we adopted a large repertoire of connectivity estimators including our novel approach, which is one of the first techniques that can uncover the strength, direction, and lag between different frequencies. We successfully discriminated correct and wrong answers based on FCGs tabulating the interactions between F^{θ} and $PO^{\alpha}{}_2$ estimated with the novel dSTE. Zero time-lag between bilateral F^{θ} and right $PO^{\alpha}{}_2$ could also indicate mental calculation performance independently of task difficulty. Overall, our results highlight the significant role of integrated activity between F^{θ} and $PO^{\alpha}{}_2$ via the strength of their causal interactions and the precise timing of their coordination for arithmetic performance.

AUTHOR CONTRIBUTIONS

Conception of the research: SD. Methods design and data analysis: SD. Drafting the manuscript: SD. Critical revision of the manuscript: YS, NT, and AB.

ACKNOWLEDGMENTS

This work was supported in part by the National University of Singapore for Cognitive Engineering Group at the Singapore Institute for Neurotechnology under grant R-719-001-102-232,

Ministry of Education of Singapore under the grant MOE2014-T2-1-115, and Temasek Laboratories Research Collaboration under the grant R-581-000-093-422 awarded to T.B. Penney. The authors would also like to acknowledge the assistance of B. Rebsamen in EEG data collection.

SUPPLEMENTARY MATERIAL

The Supplementary Material for this article can be found online at: http://journal.frontiersin.org/article/10.3389/fnhum.2016.00454

REFERENCES

Adamos, D. A., Dimitriadis, S., and Laskaris, N. (2016). Towards the bio-personalization of music recommendation systems: a single-sensor EEG biomarker of subjective music preference. *Inf. Sci.* 343, 94–108. doi: 10.1016/j.ins.2016.01.005

Adhikari, A., Sigurdsson, T., Topiwala, M. A., and Gordon, J. A. (2010). Cross-correlation of instantaneous amplitudes of field potential oscillations: a straightforward method to estimate the directionality and lag between brain areas. *J. Neurosci. Methods* 191, 191–200. doi: 10.1016/j.jneumeth.2010.06.019

Antonakakis, M., Dimitriadis, S. I., Zervakis, M., Micheloyannis, S., Rezaie, R., Babajani-Feremi, A., et al. (2016). Altered cross-frequency coupling in resting-state MEG after mild traumatic brain injury. *Int. J. Psychophysiol.* 102, 1–11. doi: 10.1016/j.ijpsycho.2016.02.002

Asada, H., Fukuda, Y., Tsunoda, S., Yamaguchi, M., and Tonoike, M. (1999). Frontal midline theta rhythms reflect alternative activation of prefrontal cortex and anterior cingulate cortex in humans. *Neurosci. Lett.* 274, 29–32. doi: 10.1016/S0304-3940(99)00679-5

Awh, E., Vogel, E. K., and Oh, S. H. (2006). Interactions between attention and working memory. *Neuroscience* 139, 201–208. doi: 10.1016/j.neuroscience.2005.08.023

Baddeley, A. (1992). Working memory: the interface between memory and cognition. *J. Cogn. Neurosci.* 4, 281–288.

Barnett, L., and Seth, A. K. (2014). The MVGC multivariate Granger causality toolbox: a new approach to Granger-causal inference. *J. Neurosci. Methods* 223, 50–68. doi: 10.1016/j.jneumeth.2013.10.018 ISSN 0165-0270.

Başar, E., Düzgün, A., Güntekin, B. (2014). A proposal to extend Brodmann's areas concept to a new model. *Neuroquantology* 12, 201–209. doi: 10.14704/nq.2014.12.2.745

Benjamini, Y., and Hochberg, Y. (1995). Controlling the false discovery rate: a practical and powerful approach to multiple testing. *J. R. Stat. Soc. Ser. B* 57, 289–300.

Brass, M., Ullsperger, M., Knoesche, T. R., von Cramon, D. Y., and Phillips, N. A. (2005). Who comes first? The role of the prefrontal and parietal cortex in cognitive control. *J. Cogn. Neurosci.* 17, 1367–1375.

Buchel, C., and Friston, K. J. (1997). Modulation of connectivity in visual pathways by attention: cortical interactions evaluated with structural equation modelling and fMRI. *Cereb. Cortex* 7, 768–778. doi: 10.1093/cercor/7.8.768

Bush, G., Luu, P., and Posner, M. I. (2000). Cognitive and emotional influences in anterior cingulate cortex. *Trends Cogn. Sci.* 4, 215–222. doi: 10.1016/S1364-6613(00)01483-2

Carreiras, M., Monahan, P. J., Lizarazu, M., Dunabeitia, J. A., and Molinaro, N. (2015). Numbers are not like words: different pathways for literacy and numeracy. *Neuroimage* 118, 79–89. doi: 10.1016/j.neuroimage.2015.06.021

Chik, D. (2013). Theta-alpha cross-frequency synchronization facilitates working memory control – a modeling study. *Springerplus* 2, 14. doi: 10.1186/2193-1801-2-14

Chochon, F., Cohen, L., van de Moortele, P. F., and Dehaene, S. (1999). Differential contributions of the left and right inferior parietal lobules to number processing. *J. Cogn. Neurosci.* 11, 617–630. doi: 10.1162/089892999563689

Chun, M. M. (2011). Visual working memory as visual attention sustained internally over time. *Neuropsychologia* 49, 1407–1409. doi: 10.1016/j.neuropsychologia.2011.01.029

Cohen, J. D., Perlstein, W. M., Braver, T. S., Nystrom, L. E., Noll, D. C., Jonides, J., et al. (1997). Temporal dynamics of brain activation during a working memory task. *Nature* 386, 604–608. doi: 10.1038/386604a0

Cohen, M. X. (2008). Assessing transient cross-frequency coupling in EEG data. *J. Neurosci. Methods* 168, 494–499. doi: 10.1016/j.jneumeth.2007.10.012

Corbetta, M., and Shulman, G. L. (2002). Control of goal-directed and stimulus-driven attention in the brain. *Nat. Rev. Neurosci.* 3, 201–215. doi: 10.1038/nrn755

Crowe, D. A., Goodwin, S. J., Blackman, R. K., Sakellaridi, S., Sponheim, S. R., MacDonald, A. W., et al. (2013). Prefrontal neurons transmit signals to parietal neurons that reflect executive control of cognition. *Nat. Neurosci.* 16, 1484–1491. doi: 10.1038/nn.3509

Curtis, C. E., and D'Esposito, M. (2003). Persistent activity in the prefrontal cortex during working memory. *Trends Cogn. Sci.* 7, 415–423. doi: 10.1016/S1364-6613(03)00197-9

Daunizeau, J., David, O., and Stephan, K. E. (2011). Dynamic causal modelling: a critical review of the biophysical and statistical foundations. *Neuroimage* 58, 312–322. doi: 10.1016/j.neuroimage.2009.11.062

David, O., Kiebel, S. J., Harrison, L., Mattout, J., Kilner, J., and Friston, K. J. (2006). Dynamic causal modelling of evoked responses in EEG and MEG. *Neuroimage* 30, 1255–1272. doi: 10.1016/j.neuroimage.2005.10.045

De Smedt, B., Grabner, R. H., and Studer, B. (2009). Oscillatory EEG correlates of arithmetic strategy use in addition and subtraction. *Exp. Brain Res.* 195, 635–642. doi: 10.1007/s00221-009-1839-9

Dehaene, S., and Cohen, L. (1997). Cerebral pathways for calculation: double dissociation between rote verbal and quantitative knowledge of arithmetic. *Cortex* 33, 219–250. doi: 10.1016/S0010-9452(08)70002-9

Dehaene, S., Molko, N., Cohen, L., and Wilson, A. J. (2004). Arithmetic and the brain. *Curr. Opin. Neurobiol.* 14, 218–224. doi: 10.1016/j.conb.2004.03.008

Dehaene, S., Piazza, M., Pinel, P., and Cohen, L. (2003). Three parietal circuits for number processing. *Cogn. Neuropsychol.* 20, 487–506. doi: 10.1080/02643290244000239

Della Puppa, A., De Pellegrin, S., d'Avella, E., Gioffre, G., Munari, M., Saladini, M., et al. (2013). Right parietal cortex and calculation processing: intraoperative functional mapping of multiplication and addition in patients affected by a brain tumor. *J. Neurosurg.* 119, 1107–1111. doi: 10.3171/2013.6.JNS122445

Delorme, A., and Makeig, S. (2004). EEGLAB: an open source toolbox for analysis of single-trial EEG dynamics including independent component analysis. *J. Neurosci. Methods* 134, 9–21. doi: 10.1016/j.jneumeth.2003.10.009

Delorme, A., Westerfield, M., and Makeig, S. (2007). Medial prefrontal theta bursts precede rapid motor responses during visual selective attention. *J. Neurosci.* 27, 11949–11959. doi: 10.1523/JNEUROSCI.3477-07.2007

Desimone, R., and Duncan, J. (1995). Neural mechanisms of selective visual attention. *Annu. Rev. Neurosci.* 18, 193–222. doi: 10.1146/annurev.ne.18.030195.001205

D'Esposito, M., and Postle, B. R. (2015). The cognitive neuroscience of working memory. *Annu. Rev. Psychol.* 66, 115–142. doi: 10.1146/annurev-psych-010814-015031

Dimitriadis, S., Sun, Y., Laskaris, N., Thakor, N., and Bezerianos, A. (2016a). Revealing cross-frequency causal interactions during a mental arithmetic task through symbolic transfer entropy: a novel vector-quantization approach. *IEEE Trans. Neural Syst. Rehabil. Eng.* doi: 10.1109/TNSRE.2016.2516107 [Epub ahead of print].

Dimitriadis, S. I., Kanatsouli, K., Laskaris, N. A., Tsirka, V., Vourkas, M., and Micheloyannis, S. (2012). Surface EEG shows that functional segregation via phase coupling contributes to the neural substrate of mental calculations. *Brain Cogn.* 80, 45–52. doi: 10.1016/j.bandc.2012.04.001

Dimitriadis, S. I., Laskaris, N. A., Bitzidou, M. P., Tarnanas, I., and Tsolaki, M. N. (2015a). A novel biomarker of amnestic MCI based on dynamic cross-frequency coupling patterns during cognitive brain responses. *Front. Neurosci.* 9:350. doi: 10.3389/fnins.2015.00350

Dimitriadis, S. I., Laskaris, N. A., and Micheloyannis, S. (2015b). Dynamics of EEG-based network microstates unmask developmental and task differences during mental arithmetic and resting wakefulness. *Cogn. Neurodyn.* 9, 371–387. doi: 10.1007/s11571-015-9330-8

Dimitriadis, S. I., Laskaris, N. A., Simos, P. G., Fletcher, J. M., and Papanicolaou, A. C. (2016b). Greater repertoire and temporal variability of cross-frequency coupling (CFC) modes in resting-state neuromagnetic recordings among children with reading difficulties. *Front. Hum. Neurosci.* 10:163. doi: 10.3389/fnhum.2016.00163

Dimitriadis, S. I., Laskaris, N. A., Tsirka, V., Vourkas, M., Micheloyannis, S., and Fotopoulos, S. (2010). Tracking brain dynamics via time-dependent network analysis. *J. Neurosci. Methods* 193, 145–155. doi: 10.1016/j.jneumeth.2010.08.027

Dimitriadis, S. I., Sun, Y., Kwok, K., Laskaris, N. A., and Bezerianos, A. (2013). A tensorial approach to access cognitive workload related to mental arithmetic from EEG functional connectivity estimates. *Conf. Proc. IEEE Eng. Med. Biol. Soc.* 2013, 2940–2943. doi: 10.1109/EMBC.2013.6610156

Dimitriadis, S. I., Sun, Y., Kwok, K., Laskaris, N. A., Thakor, N., and Bezerianos, A. (2015c). Cognitive workload assessment based on the tensorial treatment of EEG estimates of cross-frequency phase interactions. *Ann. Biomed. Eng.* 43, 977–989. doi: 10.1007/s10439-014-1143-0

Dimitriadis, S. I., Zouridakis, G., Rezaie, R., Babajani-Feremi, A., and Papanicolaou, A. C. (2015d). Functional connectivity changes detected with magnetoencephalography after mild traumatic brain injury. *Neuroimage Clin.* 9, 519–531. doi: 10.1016/j.nicl.2015.09.011

Downey, R., and Hirschfeldt, D. R. (2010). *Algorithmic Randomness, and Complexity*. Berlin: Springer.

Enriquez-Geppert, S., Huster, R. J., Figge, C., and Herrmann, C. S. (2014). Self-regulation of frontal-midline theta facilitates memory updating and mental set shifting. *Front. Behav. Neurosci.* 8:420. doi: 10.3389/fnbeh.2014.00420

Fehr, T., Code, C., and Herrmann, M. (2007). Common brain regions underlying different arithmetic operations as revealed by conjunct fMRI-BOLD activation. *Brain Res.* 1172, 93–102. doi: 10.1016/j.brainres.2007.07.043

Fell, J., and Axmacher, N. (2011). The role of phase synchronization in memory processes. *Nat. Rev. Neurosci.* 12, 105–118. doi: 10.1038/nrn2979

Feredoes, E., Heinen, K., Weiskopf, N., Ruff, C., and Driver, J. (2011). Causal evidence for frontal involvement in memory target maintenance by posterior brain areas during distracter interference of visual working memory. *Proc. Natl. Acad. Sci. U.S.A.* 108, 17510–17515. doi: 10.1073/pnas.1106439108

Fries, P. (2005). A mechanism for cognitive dynamics: neuronal communication through neuronal coherence. *Trends Cogn. Sci.* 9, 474–480.

Friese, U., Koster, M., Hassler, U., Martens, U., Trujillo-Barreto, N., and Gruber, T. (2013). Successful memory encoding is associated with increased cross-frequency coupling between frontal theta and posterior gamma oscillations in human scalp-recorded EEG. *Neuroimage* 66, 642–647. doi: 10.1016/j.neuroimage.2012.11.002

Friston, K. J. (2011). Functional and effective connectivity: a review. *Brain Connect.* 1, 13–36. doi: 10.1089/brain.2011.0008

Friston, K. J., Harrison, L., and Penny, W. D. (2003). Dynamic causal modelling. *Neuroimage* 19, 1273–1302. doi: 10.1016/S1053-8119(03)00202-7

Furl, N., Coppola, R., Averbeck, B. B., and Weinberger, D. R. (2013). Cross-frequency power coupling between hierarchically organized face-selective areas. *Cereb. Cortex* doi: 10.1093/cercor/bht097 [Epub ahead of print].

Gazzaley, A., and D'Esposito, M. (2007). Top-down modulation and normal aging. *Ann. N. Y. Acad. Sci.* 1097, 67–83. doi: 10.1196/annals.1379.010

Gobel, S. M., Calabria, M., Farne, A., and Rossetti, Y. (2006). Parietal rTMS distorts the mental number line: simulating 'spatial' neglect in healthy subjects. *Neuropsychologia* 44, 860–868. doi: 10.1016/j.neuropsychologia.2005.09.007

Grabner, R. H., and De Smedt, B. (2011). Neurophysiological evidence for the validity of verbal strategy reports in mental arithmetic. *Biol. Psychol.* 87, 128–136. doi: 10.1016/j.biopsycho.2011.02.019

Graham, J. M. (2008). The general linear model as structural equation modeling. *J. Educ. Behav. Stat.* 33, 485–506. doi: 10.3102/1076998607306151

Granger, C. W. J. (1969). Investigating causal relations by econometric models and cross-spectral methods. *Econometrica* 37, 424–438. doi: 10.2307/1912791

Grent-'t-Jong, T., and Woldorff, M. G. (2007). Timing and sequence of brain activity in top-down control of visual-spatial attention. *PLoS Biol.* 5:e12. doi: 10.1371/journal.pbio.0050012

Gruber, O., Indefrey, P., Steinmetz, H., and Kleinschmidt, A. (2001). Dissociating neural correlates of cognitive components in mental calculation. *Cereb. Cortex* 11, 350–359. doi: 10.1093/cercor/11.4.350

Harding, I. H., Yucel, M., Harrison, B. J., Pantelis, C., and Breakspear, M. (2015). Effective connectivity within the frontoparietal control network differentiates cognitive control and working memory. *Neuroimage* 106, 144–153. doi: 10.1016/j.neuroimage.2014.11.039

He, X., Cai, D., and Niyogi, P. (2005). "Laplacian score for feature selection," in *Proceeding of the Advances in Neural Information Processing Systems*, (Cambridge, MA: MIT Press), 507–514.

Higo, T., Mars, R. B., Boorman, E. D., Buch, E. R., and Rushworth, M. F. S. (2011). Distributed and causal influence of frontal operculum in task control. *Proc. Natl. Acad. Sci. U.S.A.* 108, 4230–4235. doi: 10.1073/pnas.1013361108

Hubbard, E. M., Piazza, M., Pinel, P., and Dehaene, S. (2005). Interactions between number and space in parietal cortex. *Nat. Rev. Neurosci.* 6, 435–448. doi: 10.1038/nrn1684

Hubbard, E. M., Piazza, M., Pinel, P., and Dehaene, S. (2009). "Numerical and spatial intuitions: a role for posterior parietal cortex," in *Cognitive Biology: Evolutionary and Developmental Perspectives on Mind, Brain and Behavior*, eds L. Tommasi, L. Nadel, and M. A. Peterson (Cambridge, MA: MIT Press), 221–246.

Ischebeck, A., Zamarian, L., Schocke, M., and Delazer, M. (2009). Flexible transfer of knowledge in mental arithmetic–an fMRI study. *Neuroimage* 44, 1103–1112. doi: 10.1016/j.neuroimage.2008.10.025

Ishihara, T., and Yoshi, N. (1972). Multivariate analytic study of EEG and mental activity in juvenile delinquents. *Electroencephalogr. Clin. Neurophysiol.* 33, 71–80. doi: 10.1016/0013-4694(72)90026-0

Ishii, R., Canuet, L., Ishihara, T., Aoki, Y., Ikeda, S., Hata, M., et al. (2014). Frontal midline theta rhythm and gamma power changes during focused attention on mental calculation: an MEG beamformer analysis. *Front. Hum. Neurosci.* 8:406. doi: 10.3389/fnhum.2014.00406

Jensen, O., and Tesche, C. D. (2002). Frontal theta activity in humans increases with memory load in a working memory task. *Eur. J. Neurosci.* 15, 1395–1399. doi: 10.1046/j.1460-9568.2002.01975.x

Kaminski, M., Ding, M., Truccolo, W. A., and Bressler, S. L. (2001). Evaluating causal relations in neural systems: granger causality, directed transfer function and statistical assessment of significance. *Biol. Cybern.* 85, 145–157. doi: 10.1007/s004220000235

Kane, M. J., and Engle, R. W. (2002). The role of prefrontal cortex in working-memory capacity, executive attention, and general fluid intelligence: an individual-differences perspective. *Psychon. Bull. Rev.* 9, 637–671. doi: 10.3758/BF03196323

Kawasaki, M., Kitajo, K., and Yamaguchi, Y. (2010). Dynamic links between theta executive functions and alpha storage buffers in auditory and visual working memory. *Eur. J. Neurosci.* 31, 1683–1689. doi: 10.1111/j.1460-9568.2010.07217.x

Kawasaki, M., and Watanabe, M. (2007). Oscillatory gamma and theta activity during repeated mental manipulations of a visual image. *Neurosci. Lett.* 422, 141–145. doi: 10.1016/j.neulet.2007.04.079

Kawasaki, M., Watanabe, M., Okuda, J., and Sakagami, M. (2006). SFS for feature selective maintenance, IPS for simple maintenance in visual working memory. *J. Vis.* 6:1100.

Kiebel, S. J., David, O., and Friston, K. J. (2006). Dynamic causal modelling of evoked responses in EEG/MEG with lead-field parameterization. *Neuroimage* 30, 1273–1284. doi: 10.1016/j.neuroimage.2005.12.055

Klimesch, W. (1999). EEG alpha and theta oscillations reflect cognitive and memory performance: a review and analysis. *Brain Res. Rev.* 29, 169–195. doi: 10.1016/S0165-0173(98)00056-3

Klimesch, W., Freunberger, R., Sauseng, P., and Gruber, W. (2008). A short review of slow phase synchronization and memory: evidence for control processes in different memory systems? *Brain Res.* 1235, 31–44. doi: 10.1016/j.brainres.2008.06.049

Kong, J., Wang, C., Kwong, K., Vangel, M., Chua, E., and Gollub, R. (2005). The neural substrate of arithmetic operations and procedure complexity. *Cogn. Brain Res.* 22, 397–405. doi: 10.1016/j.cogbrainres.2004.09.011

Lachaux, J. P., Rodriguez, E., Martinerie, J., and Varela, F. J. (1999). Measuring phase synchrony in brain signals. *Hum. Brain Mapp.* 8,

194–208. doi: 10.1002/(SICI)1097-0193(1999)8:4<194::AID-HBM4>3.0.CO;2-C

Maunsell, J. H., and Treue, S. (2006). Feature-based attention in visual cortex. *Trends Neurosci.* 29, 317–322. doi: 10.1016/j.tins.2006.04.001

McIntosh, A. R., and Mišić, B. (2013). Multivariate statistical analyses for neuroimaging data. *Annu. Rev. Psychol.* 64, 499–525. doi: 10.1146/annurev-psych-113011-143804

Menon, V., Rivera, S. M., White, C. D., Glover, G. H., and Reiss, A. L. (2000). Dissociating prefrontal and parietal cortex activation during arithmetic processing. *Neuroimage* 12, 357–365. doi: 10.1006/nimg.2000.0613

Micheloyannis, S., Sakkalis, V., Vourkas, M., Stam, C. J., and Simos, P. G. (2005). Neural networks involved in mathematical thinking: evidence from linear and non-linear analysis of electroencephalographic activity. *Neurosci. Lett.* 373, 212–217. doi: 10.1016/j.neulet.2004.10.005

Miller, B. T., and D'Esposito, M. (2005). Searching for "the top" in top-down control. *Neuron* 48, 535–538. doi: 10.1016/j.neuron.2005.11.002

Miller, B. T., Vytlacil, J., Fegen, D., Pradhan, S., and D'Esposito, M. (2011). The prefrontal cortex modulates category selectivity in human extrastriate cortex. *J. Cogn. Neurosci.* 23, 1–10. doi: 10.1162/jocn.2010.21516

Miller, E. K., and Cohen, J. D. (2001). An integrative theory of prefrontal cortex function. *Annu. Rev. Neurosci.* 24, 167–202. doi: 10.1146/annurev.neuro.24.1.167

Mitchell, D. J., and Cusack, R. (2008). Flexible, capacity-limited activity of posterior parietal cortex in perceptual as well as visual short-term memory tasks. *Cereb. Cortex* 18, 1788–1798. doi: 10.1093/cercor/bhm205

Mizuhara, H., Wang, L. Q., Kobayashi, K., and Yamaguchi, Y. (2004). A long-range cortical network emerging with theta oscillation in a mental task. *Neuroreport* 15, 1233–1238. doi: 10.1097/01.wnr.0000126755.09715.b3

Moran, R. J., Kiebel, S. J., Stephan, K. E., Reilly, R. B., Daunizeau, J., and Friston, K. J. (2007). Aneural mass model of spectral responses in electrophysiology. *Neuroimage* 37, 706–720. doi: 10.1016/j.neuroimage.2007.05.032

Moran, R. J., Stephan, K. E., Kiebel, S. J., Rombach, M., O'Connor, W. T., Murphy, K. J., et al. (2008). Bayesian estimation of synaptic physiology from the spectral responses of neural masses. *Neuroimage* 42, 272–284. doi: 10.1016/j.neuroimage.2008.01.025

Moran, R. J., Stephan, K. E., Seidenbecher, T., Pape, H. C., Dolan, R. J., and Friston, K. J. (2009). Dynamic causal models of steady-state responses. *Neuroimage* 44, 796–811. doi: 10.1016/j.neuroimage.2008.09.048

Musall, S., von Pfostl, V., Rauch, A., Logothetis, N. K., and Whittingstall, K. (2014). Effects of neural synchrony on surface EEG. *Cereb. Cortex* 24, 1045–1053. doi: 10.1093/cercor/bhs389

Ng, B. S., Logothetis, N. K., and Kayser, C. (2013). EEG phase patterns reflect the selectivity of neural firing. *Cereb. Cortex* 23, 389–398. doi: 10.1093/cercor/bhs031

Olson, I. R., and Berryhill, M. (2009). Some surprising findings on the involvement of the parietal lobe in human memory. *Neurobiol. Learn. Mem.* 91, 155–165. doi: 10.1016/j.nlm.2008.09.006

Onton, J., Westerfield, M., Townsend, J., and Makeig, S. (2006). Imaging human EEG dynamics using independent component analysis. *Neurosci. Biobehav. Rev.* 30, 808–822. doi: 10.1016/j.neubiorev.2006.06.007

Palva, J. M., Palva, S., and Kaila, K. (2005). Phase synchrony among neuronal oscillations in the human cortex. *J. Neurosci.* 25, 3962–3972. doi: 10.1523/JNEUROSCI.4250-04.2005

Palva, S., and Palva, J. M. (2012). Discovering oscillatory interaction networks with M/EEG: challenges and breakthroughs. *Trends Cogn. Sci.* 16, 219–230. doi: 10.1016/j.tics.2012.02.004

Papana, A., Kyrtsou, C., Kugioumtzis, D., and Diks, C. (2013). Simulation study of direct causality measures in multivariate time series. *Entropy* 2013, 2635–2661. doi: 10.3390/e15072635

Penny, W. D., Stephan, K. E., Mechelli, A., and Friston, K. J. (2004a). Modelling functional interaction: a comparison of structural equation and dynamic causal models. *Neuroimage* 23, 264–274. doi: 10.1016/j.neuroimage.2004.07.041

Penny, W. D., Stephan, K. E., Mechelli, A., and Friston, K. J. (2004b). Comparing dynamic causal models. *Neuroimage* 22, 1157–1172. doi: 10.1016/j.neuroimage.2004.03.026

Pinel, P., Piazza, M., Le Bihan, D., and Dehaene, S. (2004). Distributed and overlapping cerebral representations of number, size, and luminance during comparative judgments. *Neuron* 41, 983–993. doi: 10.1016/S0896-6273(04)00107-2

Postle, B. R. (2006). Working memory as an emergent property of the mind and brain. *Neuroscience* 139, 23–38. doi: 10.1016/j.neuroscience.2005.06.005

Postle, B. R., Berger, J. S., and D'Esposito, M. (1999). Functional neuroanatomical double dissociation of mnemonic and executive control processes contributing to working memory performance. *Proc. Natl. Acad. Sci. U.S.A.* 96, 12959–12964. doi: 10.1073/pnas.96.22.12959

Reynolds, J. H., and Chelazzi, L. (2004). Attentional modulation of visual processing. *Annu. Rev. Neurosci.* 27, 611–647. doi: 10.1146/annurev.neuro.26.041002.131039

Romero, S., Mananas, M. A., and Barbanoj, M. J. (2008). A comparative study of automatic techniques for ocular artifact reduction in spontaneous EEG signals based on clinical target variables: a simulation case. *Comput. Biol. Med.* 38, 348–360. doi: 10.1016/j.compbiomed.2007.12.001

Roux, F., and Uhlhaas, P. J. (2014). Working memory and neural oscillations: alpha-gamma versus theta-gamma codes for distinct WM information? *Trends Cogn. Sci.* 18, 16–25. doi: 10.1016/j.tics.2013.10.010

Rowe, J. B., Toni, I., Josephs, O., Frackowiak, R. S., and Passingham, R. E. (2000). The prefrontal cortex: response selection or maintenance within working memory? *Science* 288, 1656–1660. doi: 10.1126/science.288.5471.1656

Sakai, K., and Passingham, R. E. (2003). Prefrontal interactions reflect future task operations. *Nat. Neurosci.* 6, 75–81. doi: 10.1038/nn987

Sasaki, K., Tsujimoto, T., Nishikawa, S., Nishitani, N., and Ishihara, T. (1996). Frontal mental theta wave recorded simultaneously with magnetoencephalography and electroencephalography. *Neurosci. Res.* 26, 79–81. doi: 10.1016/0168-0102(96)01082-6

Sauseng, P., Klimesch, W., Schabus, M., and Doppelmayr, M. (2005). Fronto-parietal EEG coherence in theta and upper alpha reflect central executive functions of working memory. *Int. J. Psychophysiol.* 57, 97–103. doi: 10.1016/j.ijpsycho.2005.03.018

Schoffelen, J. M., and Gross, J. (2009). Source connectivity analysis with MEG and EEG. *Hum. Brain Mapp.* 30, 1857–1865. doi: 10.1002/hbm.20745

Smith, E. E., and Jonides, J. (1999). Storage and executive processes in the frontal lobes. *Science* 283, 1657–1661. doi: 10.1126/science.283.5408.1657

Stam, C. J., and van Straaten, E. C. (2012). Go with the flow: use of a directed phase lag index (dPLI) to characterize patterns of phase relations in a large-scale model of brain dynamics. *Neuroimage* 62, 1415–1428. doi: 10.1016/j.neuroimage.2012.05.050

Szczepanski, S. M., Crone, N. E., Kuperman, R. A., Auguste, K. I., Parvizi, J., and Knight, R. T. (2014). Dynamic changes in phase-amplitude coupling facilitate spatial attention control in fronto-parietal cortex. *PLoS Biol.* 12:e1001936. doi: 10.1371/journal.pbio.1001936

Tallon-Baudry, C., Bertrand, O., and Fischer, C. (2001). Oscillatory synchrony between human extrastriate areas during visual short-term memory maintenance. *J. Neurosci.* 21: RC177.

Tass, P., Rosenblum, M. G., Weule, J., Kurths, J., Pikovsky, A., Volkmann, J., et al. (1998). Detection of n:m phase locking from noisy data: application to magnetoencephalography. *Phys. Rev. Lett.* 81, 3291–3294. doi: 10.1103/PhysRevLett.81.3291

Taylor, P. C., Nobre, A. C., and Rushworth, M. F. (2007). FEF TMS affects visual cortical activity. *Cereb. Cortex* 17, 391–399. doi: 10.1093/cercor/bhj156

Todd, J. J., and Marois, R. (2004). Capacity limit of visual short-term memory in human posterior parietal cortex. *Nature* 428, 751–754. doi: 10.1038/nature02466

Varela, F., Lachaux, J. P., Rodriguez, E., and Martinerie, J. (2001). The brainweb: phase synchronization and large-scale integration. *Nat. Rev. Neurosci.* 2, 229–239. doi: 10.1038/35067550

Vogel, E. K., and Machizawa, M. G. (2004). Neural activity predicts individual differences in visual working memory capacity. *Nature* 428, 748–751. doi: 10.1038/nature02447

Voytek, B., Canolty, R. T., Shestyuk, A., Crone, N. E., Parvizi, J., and Knight, R. T. (2010). Shifts in gamma phase-amplitude coupling frequency from theta to alpha over posterior cortex during visual tasks. *Front. Hum. Neurosci.* 4:191. doi: 10.3389/fnhum.2010.00191

Wager, T. D., and Smith, E. E. (2003). Neuroimaging studies of working memory: a meta-analysis. *Cogn. Affect. Behav. Neurosci.* 3, 255–274. doi: 10.3758/CABN.3.4.255

Womelsdorf, T., Johnston, K., Vinck, M., and Everling, S. (2010). Theta-activity in anterior cingulate cortex predicts task rules and their adjustments following errors. *Proc. Natl. Acad. Sci. U.S.A.* 107, 5248–5253. doi: 10.1073/pnas.0906194107

Yamada, F. (1998). Frontal midline theta rhythm and eyeblinking activity during a VDT task and a video game: useful tools for psychophysiology in ergonomics. *Ergonomics* 41, 678–688. doi: 10.1080/001401398186847

Zanto, T. P., Rubens, M. T., Thangavel, A., and Gazzaley, A. (2011). Causal role of the prefrontal cortex in top-down modulation of visual processing and working memory. *Nat. Neurosci.* 14, 656–661. doi: 10.1038/nn.2773

Conflict of Interest Statement: The authors declare that the research was conducted in the absence of any commercial or financial relationships that could be construed as a potential conflict of interest.